Available online at www.sciencedirect.com
ScienceDirect
Nuclear Instruments and Methods in Physics Research B 257 (2007) 42–46
NIM B
Beam Interactions with Materials & Atoms
www.elsevier.com/locate/nimb

Deformation, alignment and anisotropic optical properties of gold nanoparticles embedded in silica

C. Harkati Kerboua [a], J.-M. Lamarre [b], L. Martinu [b], S. Roorda [a,*]

[a] Physics Department, Université de Montréal, CP 6128, succ. Centre-ville, Montréal, Qc., Canada H3C 3J7
[b] Department of Engineering Physics, École Polytechnique de Montreal, CP 6079, succ. Centre-ville, Montréal, Qc., Canada H3C 3A7

Available online 10 January 2007

Abstract

Gold/silica composite films with single and multilayer structures were fabricated by simultaneous gold sputtering and plasma-enhanced chemical vapor deposition of SiO_2. Heating during or after deposition was performed to control particle size. Samples were irradiated, at liquid nitrogen temperature, using 15 MeV Cu^{3+} ions or 27.5 MeV In^{7+} ions. Microstructural analysis by transmission electron microscopy revealed that spherical or nearly spherical gold nanoparticles were transformed during the irradiation into prolate ellipsoids whose long axis is along the ion beam direction. The optical absorption band attributed to surface plasmon resonance of gold particles was located at 520 nm for single layer films and at 602 nm for multilayer structures. After ion irradiation, this band splits into two polarization-dependent bands whose positions strongly depend on the size, aspect ratio and alignment of the nanorods.

PACS: 61.80.Jh; 61.46.Df

Keywords: Nanocomposites; Ion irradiation; Nanorods; Surface plasmon resonance; Gold

1. Introduction

The electrical, magnetic and optical properties of nanoparticles embedded in a dielectric matrix drastically differ from the corresponding bulk properties and strongly depend on their size, shape, inter-particle distance and surrounding medium [1]. The fabrication and characterization of these materials is a very active field of research motivated by their potential applications in optical and optoelectronic devices [2,3].

Noble metal particles strongly absorb the electromagnetic field around a certain frequency in the visible region. This phenomenon is known as surface plasmon resonance (SPR) [1,4,5]. In the case of nanorods the SPR splits into two bands: a longitudinal mode along the long axis of the rod and a doubly-degenerated transversal mode along both short axes [1,3,4,6]. If the nanorods are aligned, the microstructure is anisotropic which leads to optical properties that depend on the light incidence angle and polarization.

Different methods allow the preparation of metal nanoparticles with regular and irregular shapes. This includes ion implantation [7], sputtering [8], evaporation [9], chemical and electrochemical methods [6], sol–gel [10] and hybrid techniques combining, for example, sputtering and plasma-enhanced chemical vapor deposition [11–16]. Most of these methods produce randomly oriented nanorods. Among the techniques used to obtain nanorod particles [14,17–19], ion implantation offers the advantage of allowing the control of both alignment and aspect ratio of the irradiated particles. In the present work, we have used heavy ion irradiation to tailor the shape of gold nanoparticles embedded in silica and to induce anisotropic optical properties.

2. Experimental details

Gold/dielectric nanocomposite films with single and multilayer structures were deposited onto fused silica

* Corresponding author. Tel.: +1 514 343 2076; fax: +1 514 343 7375.
E-mail address: sjoerd.roorda@umontreal.ca (S. Roorda).

0168-583X/$ - see front matter © 2006 Elsevier B.V. All rights reserved.
doi:10.1016/j.nimb.2006.12.167

substrates by a hybrid technique combining pulsed-DC gold sputtering and plasma-enhanced chemical vapor deposition (PECVD) with SiH_4/O_2 chemistry. Single layer nanocomposite Au/SiO_2 films were deposited at room temperature using a method described elsewhere [14]. Subsequent annealing at 900 °C for 9 h was used to increase the size of gold nanoparticles. To fabricate the multilayer structures, Au/SiO_2 and SiO_2 layers were deposited alternately during 3.5 s and 60 s, respectively, onto substrates heated at 340 °C. Gold was sputtered from a pure gold target in Ar using a pulse frequency of 350 kHz and a pulse length of 1.4 μs. The peak power delivered to the target was 500 W. Heating during deposition led to the growth of gold nanoparticles via surface diffusion. PECVD of SiO_2 was performed using SiH_4/O_2 chemistry with an RF input power of 40 W and a self-bias potential of −340 V. The total pressure of the three gases (Ar, O_2 and SiH_4) introduced into the reactor was 60 mTorr. Silica deposition parameters were kept constant during the growth of the Au/SiO_2 and SiO_2 layers. The samples were then irradiated, at liquid nitrogen temperature, with 27.5 MeV In^{7+} or 15 MeV Cu^{3+} ions, either perpendicularly or at an angle (ψ) of 45° with respect to the sample normal.

The gold amount was determined by Rutherford backscattering spectroscopy (RBS) using 2 MeV He^{2+} ions. Simulation spectra gave the following results: 2.1×10^{16} at./cm^2 for single layer films, and about 1.0×10^{16} at./cm^2 per layer in the multilayer structure. Transmission electron microscopy (TEM) was performed at 200 kV. TEM specimens were prepared using mechanical polishing and ion thinning. Computer software [20] was used to analyze the size and size distribution of particles.

Optical transmission spectra from 300 to 800 nm were obtained at room temperature using an ellipsometer in order to control the light polarization direction. Transmission measurements were normalized using the transmission of fused silica substrate. The geometry of the optical measurements is shown in Fig. 1. The incident angle of light (φ) and ions (ψ) are defined relative to the sample normal. The ion beam direction, the incident light direction and the surface normal are in the same plane. The electric field is parallel to this plane in P polarization and perpendicular to it in S polarization. Note that the variation of the angle φ allows one to excite the longitudinal plasmon mode, the transversal plasmon mode or both.

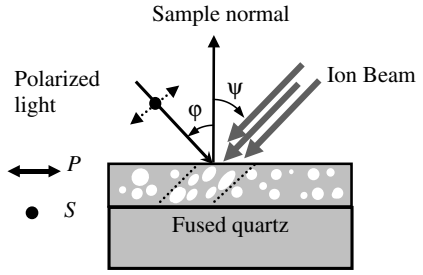

Fig. 1. Schematic representation of an irradiated sample with single layer structure. The implantation angle ψ and the light incidence angle φ are defined relative to the sample normal.

3. Results and discussion

3.1. Low gold concentration single layer structures

Fig. 2 shows cross-sectional scanning transmission electron microscopy (STEM) dark field micrographs of annealed nanocomposite films (a) before and (b) after irradiation with 15 MeV Cu^{3+} ions at a fluence of 1×10^{15} ions/cm^2. Gold nanoparticles appear bright whereas the silica matrix appears more or less dark depending on its thickness. One can see a layer of roughly spherical gold particles embedded in the silica matrix. There is also a row of gold nanoparticles at the film-substrate interface related to the procedure of preparation. In Fig. 2(a), we can observe a bimodal particle size distribution. The mean sizes of small and large particles deduced from the size distribution histogram (not shown here) are (6.0 ± 0.5) nm and (11.0 ± 0.5) nm, respectively. The thickness of the gold/silica film is about (270 ± 20) nm determined from pictures not shown here. Combining this value with RBS results, we can evaluate the gold volume fraction equal to 1.3%. The STEM picture of a perpendicularly irradiated (15 MeV Cu^{3+}, $\psi = 0°$) sample shows prolate ellipsoids (nanorods) aligned in the same direction as the ion beam (Fig. 2(b)). The spherical gold nanoparticles were deformed into ellipsoids by ion irradiation. Similar

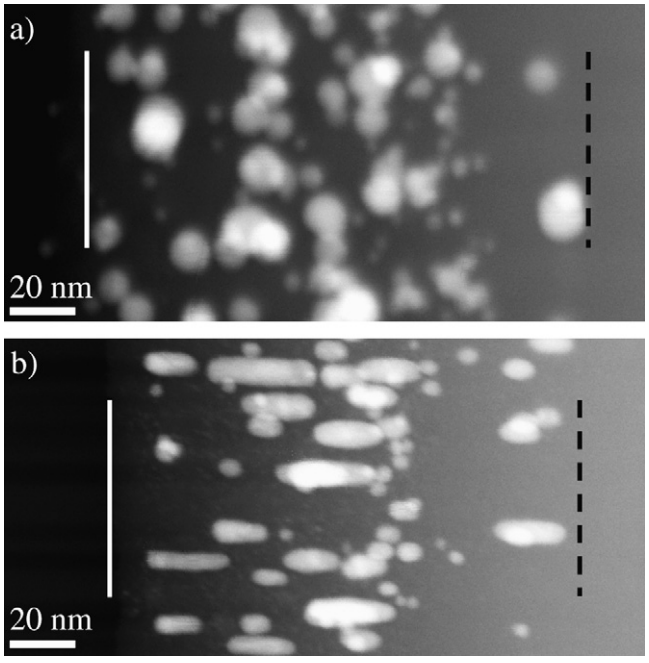

Fig. 2. Cross-sectional dark field STEM images of an annealed Au/SiO_2 nanocomposite film with single layer structure before (a) and after (b) 15 MeV Cu^{3+} irradiation with a fluence of 10^{15} ions/cm^2. Solid white line and dashed black line indicate the sample surface and the substrate-layer interface, respectively.

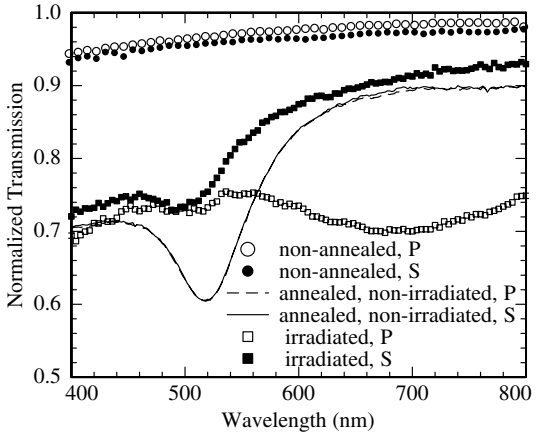

Fig. 3. P and S polarization transmission spectra of gold/silica films: as deposited, annealed non-irradiated, and annealed and irradiated with 15 MeV Cu^{3+} at a fluence of 10^{15} ions/cm^2.

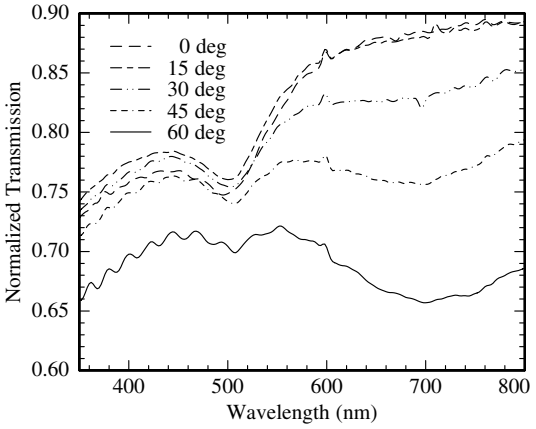

Fig. 4. P polarization transmission spectra at various incidence angles (φ) for a sample perpendicularly ($\psi = 0°$) irradiated with 15 MeV Cu^{3+} beam at a fluence of 10^{15} ions/cm^2.

deformation phenomena have been observed in irradiated gold–silica colloids [19] and Co particles embedded in bulk silica glass [21].

Optical transmission spectra corresponding to as-deposited, annealed, and annealed and irradiated samples are shown in Fig. 3 (see Fig. 1 for a description of the measurement geometry). As-deposited single layer Au/SiO_2 films show little absorption in the visible region, whereas after annealing an SPR absorption band appears around 520 nm. As a consequence, as-deposited samples are brownish but still highly transparent, while annealed samples exhibit a red-pink color. In the case of an as-grown single layer structure, the average size of metal clusters is less than 1 nm and the transmission spectra do not exhibit an absorption band. Only after the cluster size was increased (between 2 and 20 nm, see Fig. 2) can the absorption band be observed [14].

S and P polarized transmission spectra of annealed samples are identical indicating that the gold nanoparticles are spherical and thus the composite film is isotropic. For comparison, spectra of an ion beam irradiated sample measured at $\varphi = 60°$, are presented in Fig. 3. For S polarization, the spectrum shows a resonance at about 500 nm which is very close to the SPR of spherical particles. For P polarization, the SPR is separated into two bands corresponding to the oscillation of the free electrons along the short and long axes of the excited ellipsoids. The first SPR band (transversal mode) is located at (500 ± 5) nm and the second one (longitudinal mode) is at (690 ± 10) nm. These positions depend on the size and aspect ratio of the nanorods [4,6]. The blue-shift of the transversal mode is smaller than the red-shift of the longitudinal mode, in part because the small axis length changes much less than that of the long axis during deformation (see Fig. 2). The width of the longitudinal mode is relatively large, which we attribute to broadening due to the wide distribution of the aspect ratios.

Fig. 4 shows P polarization transmission measurements at different light incidence angles (φ) for a sample ion irradiated perpendicularly to its surface ($\psi = 0$). At normal light incidence, S and P transmission spectra are superimposed because they represent the optical responses of the two equivalent small axes of prolate ellipsoids (see Fig. 1). S polarization spectra (not shown here) do not exhibit special features as the angle is varied. However, P polarization curves show that the amplitude of both SPR modes (transversal and longitudinal) vary with φ. The splitting of the SPR bands is easily observed at high incidence angle ($\geqslant 30°$). The differences in the transmission amplitudes can be attributed to a change in reflectivity with φ. These observations can be explained by a simple geometrical analysis: S polarization electric field excites the short axis mode for all angles, while P polarization electric field excites both modes.

3.2. High gold concentration multilayer structures

This section reports the results obtained for Au/SiO_2 films with a multilayer structure. Fig. 5 shows selected cross-section and plan view TEM pictures of gold/silica films with multilayer structure before and after ion irradiation. The plan view (Fig. 5(a)) shows a thick region with two superimposed gold/silica layers and a thin region (beside the hole) with only one Au/SiO_2 layer. One can see that small gold particles are nearly spherical while larger ones have an irregular shape (see also Fig. 5(b)). Most gold particles are well isolated and only some of them are connected, forming large particles with an irregular shape. The first inset in Fig. 5(b) shows the electron diffraction pattern with concentric rings corresponding to (111), (200), (220) and (222) planes. This indicates polycrystalline gold, but it does not suggest any preferred plane orientation.

Closer examination of TEM images reveals that the nanoparticles are polycrystalline and that the film has a well defined multilayer structure. The second inset in Fig. 5(b) shows the particle size distribution with a Gauss-

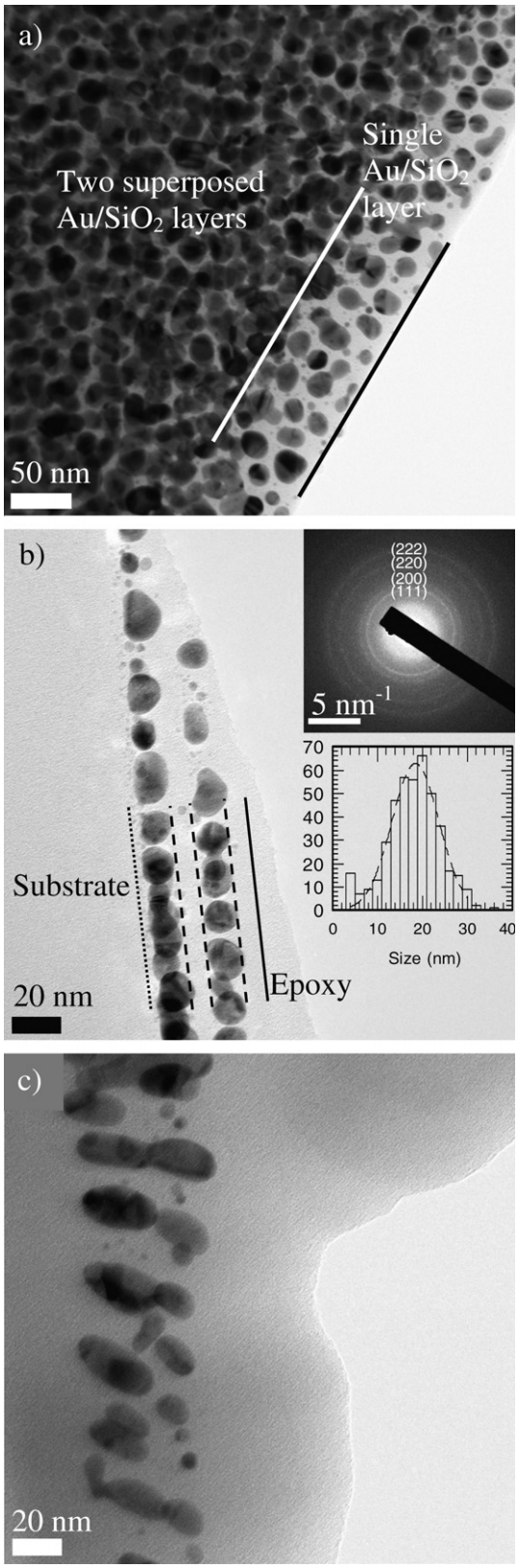

Fig. 5. (a) Plan view and (b) cross-sectional TEM images of as deposited gold/silica multilayer. The first inset in (b): electron diffraction pattern. Second inset: particle size distribution with a Gaussian fit. (c) Cross-sectional TEM micrograph of the same sample after irradiation with 2×10^{14} ions/cm^2, 27.5 MeV In^{7+} at 45° incidence.

ian fit. The mean size of gold particles is (19 ± 1) nm. In Fig. 5(b), solid, dotted and dashed lines indicate, respectively, the surface, the film-substrate interface and the interfaces between silica and gold/silica layers. The thicknesses of deposited layers were determined as follows: silica (9 ± 2) nm, gold–silica (19 ± 2) nm, silica (9 ± 2) nm and gold–silica (19 ± 2) nm for a total thickness of (56 ± 4) nm. By combining these thicknesses with the RBS results, we determine the gold volume fraction of the first (8.0%) and second (9.5%) gold–silica layers. After ion irradiation, the gold particles were deformed into prolate ellipsoids (Fig. 5(c)). The gold particles of the two layers appear aligned in the direction parallel to the ion beam and are well separated in the direction perpendicular to it. Some particles smaller than 8 nm remain spherical; this is probably related to an increasing role of surface energy as the particles get smaller.

P and S transmission spectra of gold/silica composite films with multilayer structure before and after irradiation by 27.5 MeV In^{7+} ions at a fluence of 2×10^{14} ions/cm^2 are shown in Fig. 6. The as-grown sample strongly absorbs optical radiation at 602 nm. The SPR is located at the same spectral position for P and S polarizations and its width is roughly equal to 190 nm in both cases. The width of the absorption band is related to a large distribution of particle size. After ion irradiation the longitudinal band remains close to its initial position, whereas the transversal band is blue-shifted from 602 nm to 520 nm. Moreover, the transversal band has narrowed to 100 nm.

A closer inspection of TEM pictures shows that in the direction perpendicular to the ion beam the inter-particles distances increase and their size decreases, which leads to a blue-shift of the transversal band, as observed. Dilute solutions of gold particles can appear orange, red, purple or blue as their size varies from 1 nm up to 500 nm [4,5,15,16]. As-grown samples exhibit a range of colors from pseudo-metallic gold to transparent blue in reflected

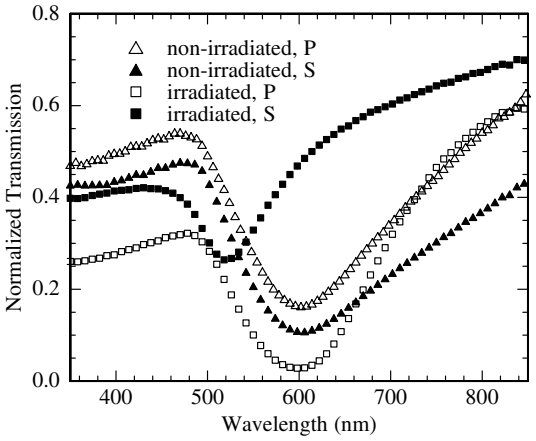

Fig. 6. P and S polarization transmission spectra ($\varphi=45°$) for as-deposited and irradiated regions using 27.5 MeV In^{7+} ions at a fluence of 2×10^{14} ions/cm^2 ($\psi=45°$).

light. After ion irradiation, the nanocomposite films change their color from blue to pink. A blue color is usually characteristic of particles larger than 60 nm. Since the particles in our samples are much smaller than this value (from 4 to 32 nm, as determined by TEM), we suggest that the small inter-particle separation leads to dipole interaction. After irradiation, this separation is larger enough (see Fig. 5(c)), leading to a weak interaction and hence giving rise to a pink color.

3.3. Comparison of SPR properties for single and multilayer films

The samples shown in this work exhibit an absorption band associated with the SPR absorption. However, the position and width of the absorption band depend on the precise microstructure of the material. For example, for the single layer sample with a relatively low gold concentration, the maximum absorption is located at 520 nm, whereas samples with a higher gold concentration exhibit a maximum at 602 nm. The size of the gold nanoparticles before annealing depends on the gold concentration and on the temperature of the substrate during deposition. Although the particle size distribution varies somewhat (2–20 and 4–32 nm, respectively) the shifts and the broadening are too large to be explained completely by the size effects, such as electron d-screening [22]. We suggest that the contribution of dipole coupling is important when the inter-particle distance is small. In fact, for composite materials, the dielectric matrix can reduce the dipole coupling between the gold particles or eliminate it completely (if the particle spacing is larger than twice the particle radius). When the spacing is reduced, which is the case for our samples with multilayer structure, dipole interactions become important and lead to the red-shift and the broadening of the plasmon band. A similar effect has been observed in gold–silica colloids with a variable silica shell thickness [5].

Both materials appear to behave in a similar fashion once exposed to ion irradiation. The multilayer samples, in spite of the small amount of silica in between the gold particles, exhibit the same deformation from spherical particles to prolate ellipsoids. SPR splitting is observed for both structures. We conclude that along the particle's short axis (S), the optical response of single and multilayer systems is similar. On the contrary, along the particle long axis (P), we observed a red-shift in the single layer structure, while no shift is apparent in the multilayer structure.

4. Conclusion

We have prepared gold/silica nanocomposite films with single and multilayer structures and different gold concentrations using a hybrid PECVD/sputtering method. Heating during or after the growth of Au/SiO_2 films allowed the gold to agglomerate into nearly spherical particles of 2–32 nm in diameter. Ion irradiation with high energy ($\geqslant 15$ MeV) heavy ions (Cu^{3+} and In^{7+}) deformed the spherical gold particles into nanorods aligned in the same direction as the ion beam. The optical properties were anisotropic and strongly depended on the polarization and the direction of the nanorods alignment. This ion bombardment approach represents an attractive method to tailor the shape, aspect ratio and alignment of the metal nanoparticles. By modifying the microstructural characteristics, one can thus control the SPR properties such as spectral position, amplitude and width.

Acknowledgements

The authors thank L. Godbout, R. Gosselin and M. Chicoine for operating the accelerators, J.-P. Masse (from $(CM)^2$ of École polytechnique de Montréal) for his help with TEM. The authors also acknowledge the financial support provided by NSERC, VRQ (NanoQuébec) and FQRNT (RQMP).

References

[1] S. Link, M.B. Mohamed, M.A. El-Sayed, J. Phys. Chem. B 103 (1999) 3073.
[2] H. Zeng, J. Qiu, Z. Ye, C. Zhu, F. Gan, J. Cryst. Growth 267 (2004) 156.
[3] S. Link, M.A. El-Sayed, J. Chem. Phys. 114 (2001) 2362.
[4] C.F. Bohren, D.R. Huffman, in: Absorption and Scattering of Light by Small Particles, Wiley, New York, 1998.
[5] P. Mulvaney, MRS Bull. 26 (2001) 1009.
[6] S. Link, M.A. El-Sayed, J. Phys. Chem. B 103 (1999) 8410.
[7] O. Pena, L. Rodriguez, J.C. Cheang-Wong, P. Santiago, A. Crespo-Sosa, E. Munoz, A. Olivier, J. Non-Cryst. Solids 352 (2006) 349.
[8] H.B. Liao, Weijia Wen, G.K.L. Wong, J. Appl. Phys. 93 (2003) 4485.
[9] B. Satpati, J. Ghatak, B. Joseph, T. Som, D. Kabiraj, B.N. Dev, P.V. Satyam, Nucl. Instr. and Meth. B 244 (2006) 278.
[10] D. Buso, M. Guglielmi, A. Martucci, G. Mattei, P. Mazzoldi, C. Sada, M.L. Post, Nanotechnology 17 (2006) 2429.
[11] D. Dalacu, L. Martinu, J. Appl. Phys. 87 (2000) 228.
[12] D. Dalacu, L. Martinu, Appl. Phys. Lett. 77 (2000) 4283.
[13] D. Dalacu, L. Martinu, J. Opt. Soc. Am. B 18 (2001) 85.
[14] J.-M. Lamarre, Z. Yu, C. Harkati, S. Roorda, L. Martinu, Thin Solid Films 479 (2005) 232.
[15] L. Martinu, Sol. Energy Mater. 15 (1987) 21.
[16] L. Martinu, H. Biederman, in: R. d'Agostino (Ed.), Plasma Deposition Treatment and Etching of Polymers, Academic Press, Boston, 1990, p. 269.
[17] B.M.I.v.d. Zande, M.R. Böhmer, L.G.J. Fokkink, C. Schonenberger, J. Phys. Chem. B 101 (1997) 852.
[18] G.L. Hornyak, C.J. Patrissi, C.R. Martin, J. Phys. Chem. B 101 (1997) 1548.
[19] S. Roorda, T. Van Dillen, A. Polman, C. Graf, A Van Blaaderen, B.J. Kooi, Adv. Mater. 16 (2004) 235.
[20] Clemex Vision™, Version 3.0, Copyright © 1990–1999, Clemex Technologies Inc.
[21] M. Gilliot, A. En Naciri, L. Johann, C. d'Orléans, D. Muller, J.P. Stoquert, J.J. Grob, Superlattices Microstruct. 36 (2004) 161.
[22] V.V. Kresin, Phys. Rev. B 51 (1995) 1844.